

Understanding the Effects of Cholesterol and Ethanol on the Stability and Morphology of Bicellar Mixtures

Weinan Zhang¹, Weitao Zhang²

¹ Guangdong Key Laboratory for Biomedical Measurements and Ultrasound Imaging, School of Biomedical Engineering, Health Science Center, Shenzhen University, Shenzhen 518060, China

² College of Life Science and Oceanography, School of Civil Engineering, Shenzhen University, Shenzhen 518060, China

Abstract. Elucidating the stability and morphology of bicellar mixtures is of great importance in the biomedical field. In this report, self-assembly cholesterol (CHOL)-containing bicellar mixtures were investigated, that were composed of long chain hydrogenated soybean phospholipids (HSPC), short chain 1, 2-diheptanoyl-sn-glycero-3-phosphocholine (DHPC) phospholipids, negatively charged dipalmitoyl phosphatidylglycerol (1, 2-dipalmitoyl-sn-glycero-3-phospho-(1'-rac-glycerol) (DPPG), and polyethylene glycol conjugated (1, 2-dimyristoyl-sn-glycero-3-phosphoethano-lamine-N-[methoxy (polyethylene glycol)-2000] (PEG2000-DSPE) lipid. Analytical techniques like; Dynamic Light Scattering (DLS), Small Angle X-Ray Scattering (SAXS), and Transmission Electron Microscopy (TEM) were used to investigate the stability and morphology changes of these bicellar mixtures. The effects of CHOL and ethanol on the morphology and stability of these bicellar mixtures under 50°C were also studied. The transition happened from nanodiscs to nanovesicles when the CHOL molar ratio was 40% in pure water. However, adding ethanol could improve CHOL solubility when the ethanol weight ratio was 20 wt% (ethanol/lipid) that favored nanodiscs-nanovesicle transition. Additionally, the ammonium sulfate maybe another factor that could affect the morphology of these bicellar mixtures form high order d-spacing structure.

Keywords: Bicellar Mixtures; Nanodiscs; Nanovesicle; Cholesterol; Morphology and Stability.

1. Introduction

Bicellar mixtures are comprised of long and short-chain (Hydrogenated soybean phospholipids, HSPC and 1, 2-diheptanoyl-sn-glycero-3-phosphocholine, DHPC) lipids, which could self-assemble into a variety of nanostructures, such as nanodiscs, unilamellaer (ULV), and bilayer ribbons multilamellar vesicles (Katsaras et al. 2005; Kolahdouzan et al. 2017; Sut et al. 2020; Tae et al. 2022). Many applications of bicellar mixtures have been found in the biochemical and biomedical fields. First, two-cell systems are usually produced by a temperature-cycling mixture of HSPC, DHPC, charge lipids, and polyethylene glycol (PEG). The size and morphology of the two-cell systems can be controlled by the lipid concentration, mole ratio, and charge density of HSPC and DHPC (Nieh et al. 2010; Nieh et al. 2011). The advantage of this system is energy saving (no extrusion). In addition, the system is stable and not easily altered by additives. Furthermore, these systems could serve as an ideal platform for drug delivery. The HSPC/Cholesterol (CHOL)/1, 2-dimyristoyl-sn-glycero-3-phosphoethano-lamine-N-[methoxy (polyethylene glycol)-2000] (PEG2000-DSPE) liposome drug delivery system has been reported to carry the anticancer drug doxorubicin (Sun et al. 2020). As a drug carrier, bicellar has several absolute advantages than other carriers: (i) bicellar has biocompatibility and biodegradability due to phosphate lipid composition which is the main component of cell membrane, (ii) it can encapsulate hydrophobic drug and improve the circulation in vivo, (iii) the surface of bicellar could be easily modified by specific molecules and achieve the targeted delivery. For example, folic acid modification has been used in anti-cancer drug delivery system (Zhang et al. 2013; Liu et al. 2017).

Nanodiscs and nanovesicles are two possible structures of bicellar mixtures. Nanodiscs have the property of providing in vitro lipid bilayer platforms (close to natural lipid bilayer) to carry membrane proteins or collect appropriate membrane proteins directly from the cell membrane (Dolatshahi-Pirouz et al. 2011). Compared with liposomes, nanodiscs have more homogeneous (in one preparation)

and consistent (in different batches of preparation) size distribution. The more precise particle size could be controlled by adjusting the sequence length of macrophage stimulating protein (MSP). The diameter of the nanodiscs is around 10-20 nm (Dufourc 2021). Nieh et al. reported that the smaller size of nanodiscs has better permeability and uptake efficiency in cancer cells than larger sized liposomes (Truong et al. 2015). Also, the recent studies revealed that nanodiscs could be spontaneously strung with polymers in solution to form a lipid/polymer mixture, which is more efficient and stable than monomer nanodiscs. On the other hand, compared with the nanodiscs, the radius of nanovesicles is in the range of 15-50 nm, which is larger than the nanodiscs. A transition from nanodiscs to nanovesicles may occur when evaluating temperature or dilution solutions (Jin and Zheng 2011; Mulas et al. 2020).

CHOL plays a critical role in cell membrane; as the fluidity and rigidity of membrane is affected by CHOL in most of eukaryotic cells. It is widely known that CHOL is present in large quantities in the cell membranes and play a vital role. Additionally, CHOL is one of the important substances to adjust protein functions among all the components of various cell membranes and its concentration could reach approximately 50 mol%. CHOL not only regulates the physicochemical properties of lipid bilayers, such as thickness, permeability, and stiffness, but also directly regulates the allosteric modulators of membrane proteins. CHOL nanodiscs could possibly obtain its high stability and they may overcome the environment of high temperature (Yang et al. 2016; Zhang et al. 2018). Also, ethanol is widely considered an efficient osmosis enhancer, the effects of ethanol on liposome structure and the thickness of bilayer have been widely reported. This solvent is usually confirmed to affect liposome structure by increasing the bilayer fluidity and decreasing the lipid layer density (Bendas and Tadros 2007; Petelska et al. 2021). Additionally, the effects of ethanol on DHPC liposome morphology have reported that ethanol could decrease the size of the DHPC liposome (Lopez-Pinto et al. 2005). However, the effects of CHOL and ethanol on the bicellar system have never been reported. In this study, we investigated a self-assembly CHOL-containing bicellar, which was composed of HSPC, DHPC phospholipids, negatively charged DPPG, and PEGylated lipid. The interactions between CHOL and ethanol were also examined.

2. Results and Discussion

2.1 The Effects of CHOL on Bicellar Mixtures

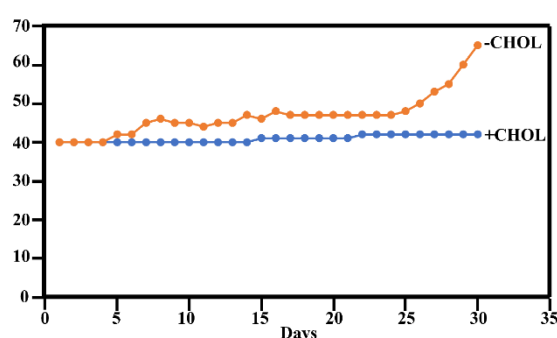


Fig 1. DLS indicates the size distribution alteration of nanodiscs involved with CHOL or without CHOL at 50 °C in 30 days.

To build a stable structure, CHOL might be placed into the midst of a two-lipid long acyl chain or into one leaflet. Therefore, at high CHOL mole fraction, unfavorable free energy dominates the mixing behavior (Fernandez et al. 2008). In order to confirm the effect of CHOL on binuclear mixtures, the HSPC/CHOL mole ratio must first be verified. Huang et al. proved that CHOL has maximum solubility in bilayer structure, which is the molar ratio lipid/CHOL=3:2 (Huang et al. 1999). We examined the 40 % CHOL molar ratio as the solubility limit in this study. We first prepared two types of nanodiscs; one with CHOL incorporated into the formulation and the other without CHOL involvement. We placed each of the two nanodiscs in a water bath at 50°C and tracked their size

distribution for 30 days (Fig. 1). The DLS data showed that in the nanodisc suspension without CHOL, the size distribution changed on the 5th day and the change continued until the 30th day, while for the nanodiscs with CHOL added to the formulation, the size distribution remained relatively uniform, and DLS data showed relatively stable size particles until the 30th day.

To further investigate the effects of CHOL on bicellar mixtures by SAXS analysis (Fig. 2). HSPC/DHPC/DPPG/PEG2000-DSPE was dissolved in pure water, HSPC/DHPC/DPPG/PEG2000-DSPE was dissolved in pure water in the presence of CHOL, HSPC/DHPC/DPPG/PEG2000-DSPE was dissolved in ammonium sulfate (250 mM), HSPC/DHPC/DPPG/PEG2000-DSPE was dissolved in ammonium sulfate (250 mM) in the presence of CHOL. First of all, we studied the CHOL effects on HSPC bicellar system in water. The HSPC/DHPC/DPPG/PEG2000-DSPE in the presence and absence of CHOL showed the same decay at low q range and one peak at high q range representing bilayer structure was formed in both samples. However, the results of the HSPC/DHPC/DPPG/PEG2000-DSPE in pure water with CHOL showed a broader peak in high q value range which indicates that morphology change might possibly be developing, this result was also confirmed by the DLS, the DLS data shows that the sample HSPC/DHPC/DPPG/PEG2000-DSPE in pure water had a peak position at 100 nm (Fig. 3A), while the sample HSPC/DHPC/DPPG/PEG2000-DSPE in the presence of CHOL peak position was at 79.5 nm (Fig. 3B). It is contradictory to the result of Lopes et al.'s work (Lopez-Pinto et al. 2005) that reported that the mean particle size in lipid composition of DPPC/CHOL was larger than DPPC samples without CHOL. Previous reports carried out by DSC (Socaciu et al. 2000) exhibited that the steroids were added into liposomes which tend to eliminate the phase-transition temperature (T_c) peak of DPPC, promotes the appearance of a new phase of vesicles, remaining in a solid state and preventing the partial dilution of the bilayers. In this study, TEM was applied to further verify the structure of HSPC/DHPC/DPPG/PEG2000-DSPE/CHOL/water samples (Fig. 4), nanovesicle structures were observed, which were correlated to SAXS and DLS results, evidencing that the transition from nanodiscs to nanovesicles could happen due to the addition of CHOL.

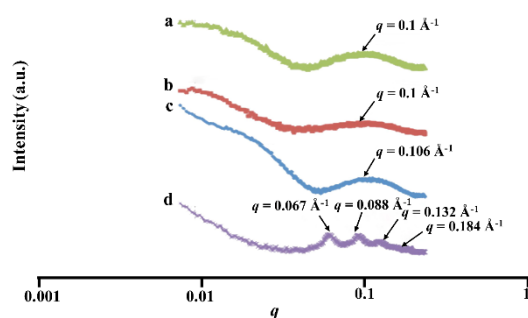


Fig 2. (a) Lipid sample with CHOL added in ammonium sulfate. (b) Lipid sample with CHOL added in pure water. (c) Lipid sample without CHOL added in ammonium sulfate. (d) Lipid sample without CHOL added in pure water.

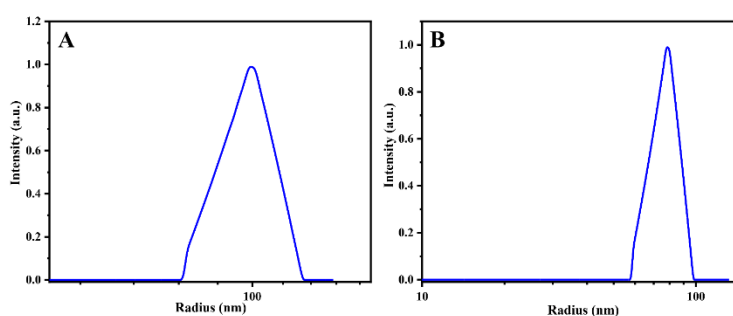


Fig 3. (A) Peak position of HSPC/DHPC/DPPG/PEG2000-DSPE was dissolved in pure water at 100 nm. (B) Peak position of HSPC/DHPC/DPPG/PEG2000-DSPE was dissolved in pure water in the presence of CHOL at 79.54 nm.

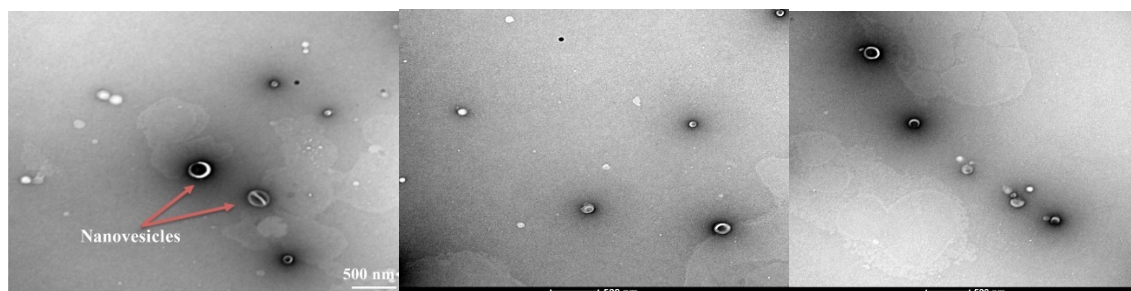


Fig 4. TEM picture of HSPC/DHPC/DPPG/PEG2000-DSPE/CHOL/water.

2.2 The Effects of CHOL with Ammonium Sulfate on Bicellar Mixtures

The SAXS data shows that four quasi-Bragg reflections peaks were detected and peaks position were $q_1=0.067 \text{ \AA}^{-1}$, $q_2=0.1 \text{ \AA}^{-1}$, $q_3=0.132 \text{ \AA}^{-1}$, and $q_4=0.184 \text{ \AA}^{-1}$, respectively. We calculated the $q_1: q_2: q_3=1:2.2:3.06$. These peak values showed an order relationship which indicated that a high order d-spacing structure has been formed. In order to confirm the possible structure, we diluted sample concentration from $C_p = 1\text{-}0.5 \text{ mg/mL}$ (Fig. 5A and 5B), the peak position did not change as the concentration was decreased, indicating that the d-spacing was stable and there was no swelling through dilution. Based on the Bragg's equation $d = 2\pi/q$, the first order spacing $d = 2\pi/0.067 = 93.73 \text{ \AA}$. This result is correlated to the work of Fernandez et al. (2008) that an initial lamellar repeat distance of around 90-100 \AA was detected in the silent dispersion of DMPG (Di-1, 4 charged lipid, 50 mM) with 250-500 mM NaCl salt solution at 25°C. It is noteworthy that DPPG (Di-1, 6) was used as a charge lipid in this study and in the study of Degovics et al. (2000), the higher-order Bragg mode will appear in DPPG with NaCl 700 mM. The DLS pattern shows mean peak position at 656.3 nm which indicates that possible huge size particles existed in this situation (Fig. 6). In the work of Roberto et al., huge MLV structures with 1 μm particle size in DMPG with an accuracy of 500 mM NaCl were also observed (Fernandez et al. 2008). Additionally, lipid film was dispersed in ammonium sulfate that already contained salt in this study, however, it has been reported that the later addition of salt will not cause multilamellar structure formed (Degovics et al. 2000), evidencing that the transformation from unilamellar to multilamellar requires a complete reorganization of the bilayers.

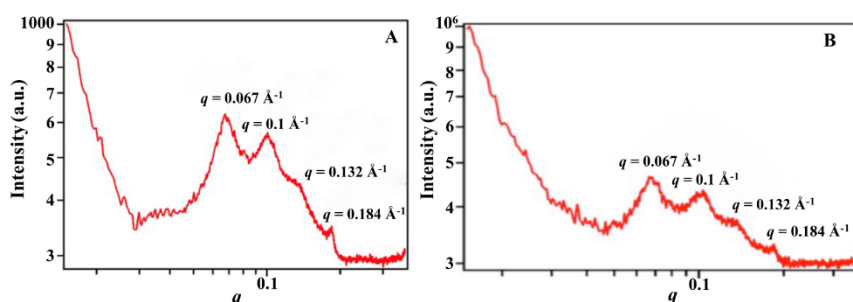


Fig 5. (A) HSPC/CHOL/salt SAXS data under $C_p = 1 \text{ mg/mL}$, (B) HSPC/CHOL/salt SAXS data under $C_p = 0.5 \text{ mg/mL}$.

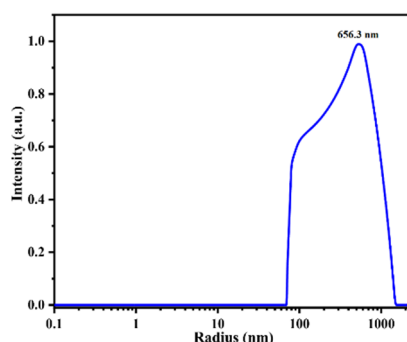


Fig 6. Mean peak position of DLS pattern at 656.3 nm.

2.3 The Effects of Long-chain/Short-chain Molar Ratio and Charge Density on Bicellar Mixtures

To form lipid/CHOL bicellar system and investigate Q value (long chain/short chain molar ratio) and R value (charge density, DPPG/whole lipid) effects on bicellar morphology, we prepared different Q value and R value samples. Q value is believed to be highly correlated with unilamellar vesicle size (van Dam et al. 2004). Additionally, R value plays a critical role in the formation of spontaneously formed ULVs and that the different morphologies are highly dependent on the balance of interactions between the various columbic repulsive, van der Waal, and hydration forces (Nieh et al. 2005). The SAXS was conducted to detect the morphology of samples (Fig. 7). SAXS pattern showed more than three Bragg reflections peaks in the high q range and a high order-spacing relationship among those peaks. Firstly, the first order peak of $q = 0.058 \text{ \AA}^{-1}$ ($d = 2\pi/q = 107.58 \text{ \AA}$) in HSPC/DHPC/DPPG/PEG2000-DSPE with $R = 0.03$, $Q = 2$ in ammonium sulfate was smaller than the HSPC/DHPC/DPPG/PEG2000-DSPE with $R = 0.05$, $Q = 2$ in salt at $q = 0.066 \text{ \AA}^{-1}$ ($d = 2\pi/q = 94.45 \text{ \AA}$). The same d-spacing peak value (d was around 100 \AA) was also reported in Roberto et al.'s work (Fernandez et al. 2008), because we proposed that high salt (250 mM ammonium sulfate) will screen the charge of DPPG to form loose multilayer structure. Also, the other peaks shifted to high q regime as well, indicating that this high order spacing layers are related to each other. The d-spacing measurement gave us the repeat distance of bilayers in stack, it combined the thickness of the bilayer and the water between the bilayers. Thus, this sequential spacing may be related to multiple layers of vesicles and a stack of double layers (e.g., hexagonal cylindrical packing). The d-spacing of layers in $R = 0.03$ sample was larger than it is in $R = 0.05$ samples. In the same way, two samples with different Q values and same R values have been examined by SAXS, the monotonic peak position of the lower-Q sample (HSPC/DHPC/DPPG/PEG2000-DSPE with $R = 0.03$ and $Q = 2$ in salt) appears at a smaller q value ($q = 0.060 \text{ \AA}^{-1}$) than that of the higher-Q sample (i.e., HSPC/DHPC/DPPG/PEG2000-DSPE with $R = 0.03$ and $Q = 3$) ($q = 0.064 \text{ \AA}^{-1}$), indicating that the d-spacing of layers was swelling as the Q value was decreasing. Furthermore, the SAXS results showed that this high-order spacing structure was unlikely to form a crystal structure because it can expand and change morphologically with different Q and R values.

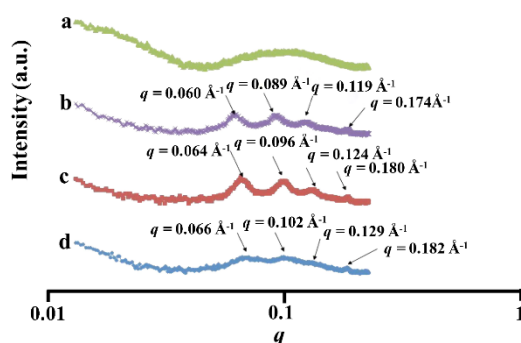


Fig 7. (a) HSPC/DHPC system without CHOL dissolved in ammonium sulfate. (b) HSPC/DHPC system $R = 0.03$, $Q = 2$ with CHOL dissolved in ammonium sulfate. (c) HSPC/DHPC system $R = 0.03$, $Q = 3$ with CHOL dissolved in ammonium sulfate. (d) HSPC/DHPC system $R = 0.05$, $Q = 2$ with CHOL dissolved in ammonium sulfate.

3. The Effects of Ethanol on Bicellar Mixtures

In order to study the effects of ethanol on the morphology of two cells, HSPC/DHPC/DPPG/PEG-2000/ ethanol solutions with different ethanol weight ratios (5 wt%, 10 wt%, and 20 wt%) were dissolved in pure water. SAXS measurements were conducted and the samples with a lipid concentration ($C_p = 10 \text{ mg/mL}$) were exhibited in Fig. 8. The SAXS data reveal same decay at low q range and a monotonic peak at high q range, indicating that a bilayer structure has been formed. Different q values ($q = 0.096 \text{ \AA}^{-1}$ in HSPC/DHPC/DPPG/PEG2000-DSPE, $q = 0.098 \text{ \AA}^{-1}$ in HSPC/DHPC/DPPG/PEG2000-DSPE/5 wt% ethanol, $q = 0.101 \text{ \AA}^{-1}$ in HSPC/ DHPC/ DPPG/ PEG

2000-DSPE/10 wt% ethanol, and $q = 0.106 \text{ \AA}^{-1}$ in HSPC/ DHPC/ DPPG/ PEG2000-DSPE/20 wt% ethanol) in four samples were observed. Followed by Bragg equation: $d = 2\pi/q$, the d spacing of these four samples were $d = 65.41 \text{ \AA}$ (none ethanol), 64.08 \AA (5 wt% ethanol), 62.17 \AA (10 wt% ethanol), 59.24 \AA (20 wt% ethanol), respectively. The SAXS result demonstrated that with an increase of ethanol weight ratio, the d -spacing of layers in these four samples was decreased. This result is correlated with Adachi's work (Ebihara et al. 1979) which indicates that the ethanol could affect lipid stiffness and fluidity, and the gel phase in phosphatidylcholine is completely staggered. The reason may be that ethanol molecules can increase the fluidity of lipids and decrease the density of the lipid layer, which may promote the interlacing of the acyl carbon chains (Barry and Gawrisch 1994; Dubey et al. 2007a; Dubey et al. 2007b). This result was consistent with the result of Lopez-Pinto's work (Lopez-Pinto et al. 2005), the presence of ethanol affects the morphology of double layer to reduce the thickness, thus decreasing the d -spacing of the bilayer.

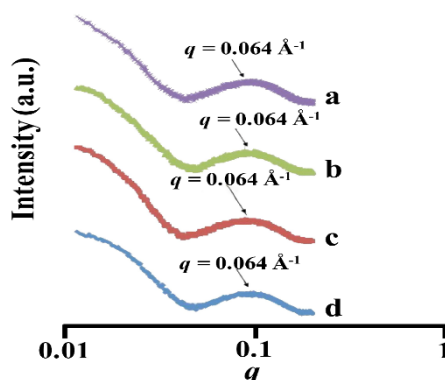


Fig 8. (a) 20 wt% ethanol in HSPC/DHPC/DPPG/PEG2000-DSPE. (b) 10 wt% ethanol in HSPC/DHPC/DPPG/PEG2000-DSPE. (c) 5 wt% ethanol in HSPC/DHPC/DPPG/PEG2000-DSPE. (d) HSPC/DHPC/DPPG/PEG2000-DSPE in water.

3.1 The Effects of Ethanol with CHOL on Bicellar Mixtures

To investigate the effects of ethanol on HSPC/DHPC/DPPG/PEG2000-DSPE/CHOL bicellar mixtures, three samples in the presence of CHOL (HSPC/CHOL=3:2 molar ratio) were prepared, the SAXS data of the mixture with lipid concentration of 10 mg/mL and ethanol weight gradient of 5 wt%, 10 wt%, and 20 wt%/ lipid were shown in Fig. 9. The results of the two initial SAXS data at 5 wt%, 10 wt%, and 20 wt%/lipid showed more than three Bragg reflection peaks, and the multi-quasi-Bragg reflection indicated that a high stratified structure might be formed, which was consistent with the results of the sample in the absence of ethanol. Most interestingly, in 20 wt% ethanol sample, the SAXS data shows that a broad peak appears from 0.05-0.2 \AA^{-1} instead of high order layers spacing peaks. DLS data (Fig. 10) on 20 wt% was conducted to confirm the size of bicellar, the mean peak position was at 31.15 nm, indicating a smaller size particle had been formed in the presence of 20 wt% ethanol than the absence of ethanol. The main reason for particle size reduction may be that ethanol could interact with the hydrophilic head group and give the surface a negative charge, and electrostatic repulsion may eventually lead to particle size reduction (Zhang et al. 2014).

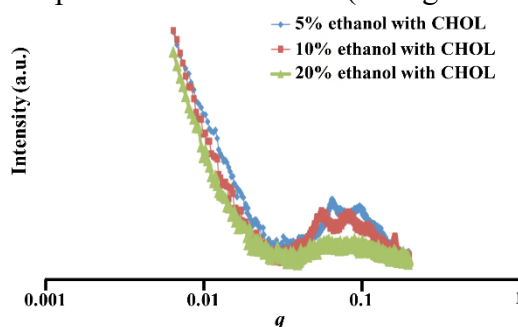


Fig 9. SAXS pattern ethanol/lipids weight 5 wt%, 10 wt%, 20 wt% dissolved in buffer solution.

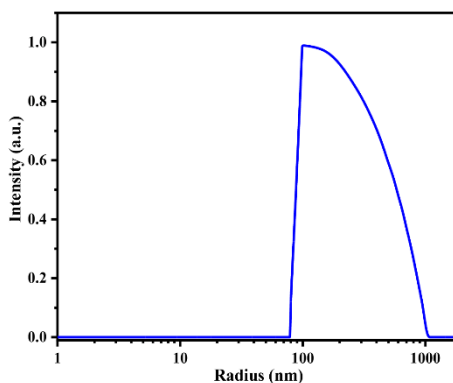


Fig 10. DLS pattern on 20wt% ethanol sample.

3.2 The Effects of Ammonium Sulfate on Bicellar Mixtures

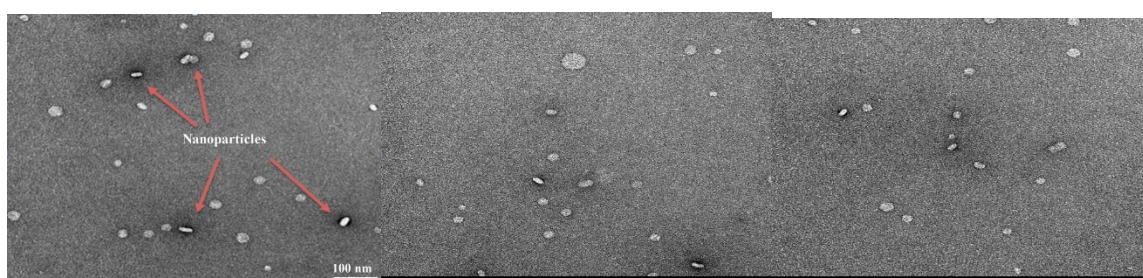


Fig 11. TEM picture HSPC/CHOL/20 wt% ethanol dissolved in water.

We prepared 20 wt% ethanol sample with CHOL dissolved in pure water. Fig. 11 shows that the disc-like structure was observed in sight field, it indicates that ethanol would effectively decrease the size of particle and favor HSPC/CHOL to form nanodisc structure. The effects of salinity on bilayer morphology have been reported (Huang et al. 1999). For the first peak, $d = 93.7 \text{ \AA}$ is correlated to previous work (Fernandez et al. 2008), the high salt solution might screen the charge of lipid (DPPG in this case), destroying the Van der Waals and repulsive interaction between the bilayer, resulting in bilayer loosening and forming multilamellar structure. For the second peak, $d = 62.8 \text{ \AA}$ is the typical bilayer structure as many articles reported, we suggested that there should be bilayer structure formed in this study. For the third and fourth peaks, d -spacing is $d = 47.7 \text{ \AA}$ and $d = 34.1 \text{ \AA}$, respectively. Therefore, the first, third and fourth peak positions are correlated to order spacing: $d_1 : d_3 : d_4 = 3 : 1.5 : 1$, indicating that the multilamellar vesicle has been formed in this study. Moreover, the DLS data shows that the particle size of the sample in the presence of ammonium sulfate is larger than that dissolved in water. This influence is possibly mainly because the ammonium sulfate effectively causes the fast coalescence to form larger sized particle which is consistent with the previous report by Ebihara et al. (1979) while contradictory with the recent report by Sarfraz et al. (2018).

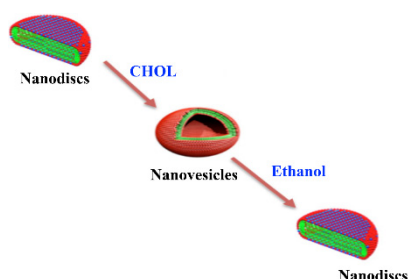


Fig 12. Diagrammatic representation of transition between nanodiscs-nanovesicles.

The high order Bragg spacing peaks were observed in the presence of CHOL and ammonium sulfate buffer solution. However, these order peaks were not found in HSPC/DHPC/DPPG/PEG2000-DSPE without CHOL in salt or with cholesterol in water, indicating that cholesterol and ammonium

sulfate could co-work to affect bicellar morphology. Additionally, the salt would have stronger interaction with dye than HSPC sample in staining. The relationship among the CHOL, ethanol, and salt is presented in Fig. 12 and Table 1.

Table 1. CHOL, ethanol, salt relationship chart

	CHOL	Ethanol	Salt	Water	Result
HSPC/DHPC/DPPG/PEG2000-DSPE	-	-	-	+	Nanodiscs
HSPC/DHPC/DPPG/PEG2000-DSPE	+	-	-	+	Nanovesicles
HSPC/DHPC/DPPG/PEG2000-DSPE	+	-	+	-	High-order spacing structure
HSPC/DHPC/DPPG/PEG2000-DSPE	-	20 wt%	-	+	Thinner layer spacing
HSPC/DHPC/DPPG/PEG2000-DSPE	+	20 wt%	+	-	Monotonic broad peak appears
HSPC/DHPC/DPPG/PEG2000-DSPE	+	20 wt%	-	+	Disc-like structure

4. Conclusion

In summary, this study provided the information that CHOL could increase the d-spacing of the layers of bicellar and enlarge the particle mean size, leading to nanodiscs-nanovesicles transition while ethanol could decrease the d-spacing of layers and favor nanovesicles-nanodiscs transition in the presence of CHOL. Additionally, the ammonium sulfate also played an important role in the formation of bicellar mixtures.

5. Materials and Methods

5.1 Materials

Table 2. Composition of individual lipids in aqueous solutions (in %)

	[HSPC]+[DPPG]+[PEG2000-DSPE]/[DHPC]-1	[HSPC]+[DPPG]+[PEG2000-DSPE]/[DHPC]-2
HSPC	74.25	66.13
DHPC	25.00	12.80
DPPG	0.75	0.63
PEG2000-DSPE	6.00	20.00
CHOL	40.00	22.00
Ethanol	20.00	-

HSPC (Hydrogenated soybean phospholipids, Mw: 783.774), DHPC (1, 2-diheptanoyl-sn-glycero-3-phosphocholine, Mw: 481.560), DPPG [1, 2-dipalmitoyl-sn-glycero-3-phospho-(1'-rac-glycerol)], and PEG2000-DSPE (1, 2-dimyristoyl-sn-glycero-3-phosphoethano-lamine-N-[methoxy (polyethylene glycol)-2000]) were provided by FormuMax (State of California, USA). Powder of ammonium sulfate was obtained from Sigma-Aldrich (St. Louis, MO, USA). The ammonium sulfate solution was prepared by dissolving 12.625 g into 500 mL pure water to make 250 mM (NH₄)₂SO₄ solution. The composition of all samples has two values: [HSPC]+[DPPG]+[PEG2000-DSPE]/[DHPC] (long chain/short chain molar ratio represented by Q), [DPPG]/[HSPC]+[DPPG]+[PEG2000-DSPE] (charge density, DPPG/whole lipid represented by R). Powder of CHOL was provided by FormuMax. Pure ethanol was taken from Self-Assemble Functional Nanomaterials Laboratory.

The total lipid concentration was 10 mg/mL in this study. Molar ratio of individual composition was different based on requirement; details are listed below (Table 2).

5.2 Dynamic Light Scattering (DLS)

The samples were performed on a compact goniometer system with multi-detectors (CGS-3MD, 22 mW He–Ne laser, a wavelength of 632.8 nm) (ALV GmbH, Langen, Germany) and four avalanche photo diode (APD) detectors evenly spaced (32°) across the tray arc driven by the goniometer. The rate constant Γ in the intensity correlation function ($e^{-2\Gamma\tau}$) could describe the single exponential decay of a single scale system. The translational diffusion coefficient (D) was related with $D = \Gamma/q^2$, where the $q = 4n\pi \times \sin(\theta/2)/\lambda$ (λ , the incident laser wavelength, n , the refractive index of the samples; θ , 90°). Based on the Stokes–Einstein $RH = KBT/6\pi\eta D$ (K , the Boltzmann constant; η , the viscosity), the hydrodynamic radius (RH) was related to D of a uniform-sized spherical particle.

5.3 Negatively Staining Transmission Electron Microscopy (TEM)

The samples were performed on a TEM at an accelerating voltage of 80 kV (FEI Tecnai T12, FEI Company, Hillsboro, USA). 4 μ L sample solutions (0.01 mg/mL) were placed on a copper grid (400-mesh) coated with formvar/carbon film (Electron Microscopy Sciences, PA, USA) and then a Whatman filter was used to soak up the excess solution. Next, the samples were negatively stained with 5 μ L uranyl acetate (10 mg/mL, SPI Supplies, PA, USA) and the filter paper was used to remove the excessive staining solution. The grid was then dried at room temperature.

5.4 Small Angle X-Ray Scattering (SAXS)

The SAXS of the samples was performed in the SAFN laboratory of the Materials Science Institute at the University of Connecticut. The intensity of X-rays scattered from a given system ($\lambda = 0.1$ nm, distance = 1300 mm). A linear position-sensitive image plate detector with resolution 250–300 μ m. The strength consists of the scattering of the lipid bilayer itself and the interactions between the particles, often referred to as the structure factor. The Bragg's equation follows the SAXS measurement of the data.

Competing Interests

The authors declare that they have no competing interest.

References

- [1] Barry JA, Gawrisch K (1994) Direct NMR evidence for ethanol binding to the lipid-water interface of phospholipid bilayers. *Biochemistry* 33:8082-8088. <https://doi.org/10.1021/bi00192a013>.
- [2] Bendas ER, Tadros MI (2007) Enhanced transdermal delivery of salbutamol sulfate via ethosomes. *Aaps Pharmscitech* 8:213-220. <https://doi.org/10.1208/pt0804107>.
- [3] Degovics G, Latal A, Lohner K (2000) X-ray studies on aqueous dispersions of dipalmitoyl phosphatidylglycerol in the presence of salt. *J Appl Crystallogr* 33:544-547. <https://doi.org/10.1107/S002188980009991X>.
- [4] Dolatshahi-Pirouz A, Nikkhah M, Kolind K, Dokmeci MR, Khademhosseini A (2011) Micro-and Nanoengineering Approaches to Control Stem Cell-Biomaterial Interactions. *J Funct Biomater* 2:88-106. <https://doi.org/10.3390/jfb2030088>.
- [5] Dubey V, Mishra D, Dutta T, Nahar M, Saraf DK, Jain NK (2007a) Dermal and transdermal delivery of an anti-psoriatic agent via ethanolic liposomes. *J Control Release* 123:148-154. <https://doi.org/10.1016/j.jconrel.2007.08.005>.
- [6] Dubey V, Mishra D, Jain NK (2007b) Melatonin loaded ethanolic liposomes: physicochemical characterization and enhanced transdermal delivery. *Eur J Pharm Biopharm* 67:398-405. <https://doi.org/10.1016/j.ejps.2010.04.005>.

- [7] Dufourc EJ (2021). Bicelles and nanodiscs for biophysical chemistry. *Biochim Biophys Acta Biomembr* 1863 (1):183478. <https://doi.org/10.1016/j.bbamem.2020.183478>.
- [8] Ebihara L, Hall JE, MacDonald RC, McIntosh TJ, Simon SA (1979) Effect of benzyl alcohol on lipid bilayers. A comparisons of bilayer systems. *Biophys J* 28:185-196.[https://doi.org/10.1016/S0006-3495\(79\)85170-X](https://doi.org/10.1016/S0006-3495(79)85170-X).
- [9] Fernandez RM, Riske KA, Amaral LQ, Itri R, Lamy MT (2008) Influence of salt on the structure of DMPG studied by SAXS and optical microscopy. *BBA-Bioenergetics* 1778:907-916.<https://doi.org/10.1016/j.bbamem.2007.12.005>.
- [10] Huang J, Buboltz JT, Feigenson GW (1999) Maximum solubility of cholesterol in phosphatidylcholine and phosphatidylethanolamine bilayers. *BBA-Bioenergetics* 1417:89-100.[https://doi.org/10.1016/S0005-2736\(98\)00260-0](https://doi.org/10.1016/S0005-2736(98)00260-0).
- [11] Jin CS, Zheng G (2011) Liposomal nanostructures for photosensitizer delivery. *Laser Surg Med* 43:734-748. <https://doi.org/10.1002/lsm.21101>.
- [12] Katsaras J, Harroun TA, Pencer J, Nieh M-P (2005) “Bicellar” lipid mixtures as used in biochemical and biophysical studies. *Naturwissenschaften* 92:355-366.<https://doi.org/10.1007/s00114-005-0641-1>.
- [13] Kolahdouzan K, Jackman JA, Yoon BK, Kim MC, Johal MS, Cho N-J (2017). Optimizing the formation of supported lipid bilayers from bicellar mixtures. *Langmuir* 33(20):5052-5064. <https://doi.org/10.1021/acs.langmuir.7b00210>.
- [14] Liu Y, Xia Y, Rad AT, Aresh W, Nieh MP (2017). Stable discoidal bicelles: a platform of lipid nanocarriers for cellular delivery. *Methods Mol Biol* 1522:273-282.https://doi.org/10.1007/978-1-4939-6591-5_22.
- [15] Lopez-Pinto JM, Gonzalez-Rodriguez ML, Rabasco AM (2005) Effect of cholesterol and ethanol on dermal delivery from DPPC liposomes. *Int J Pharmaceut* 298:1-12. <https://doi.org/10.1016/j.ijpharm.2005.02.021>.
- [16] Mulas G, Rolla GA, Geraldles CFGC, Starmans LWE, Botta M, Terreno E, Tei L (2020). Mn (II)-based lipidic nanovesicles as high-efficiency MRI probes. *ACS Appl Bio Mater* 3(4):2401-2409. <https://doi.org/10.1021/acsabm.0c00138>.
- [17] Nieh M-P, Raghunathan VA, Kline SR, Harroun TA, Huang C-Y, Pencer J, Katsaras J (2005) Spontaneously formed unilamellar vesicles with path-dependent size distribution. *Langmuir* 21:6656-6661. <https://doi.org/10.1021/la0508994>.
- [18] Nieh MP, Dolinar P, Kucerka N, Kline SR, Debeer-Schmitt LM, Littrell KC, Katsaras J (2011) Formation of kinetically trapped nanoscopic unilamellar vesicles from metastable nanodiscs. *Langmuir* 27:14308-14316. <https://doi.org/10.1021/la2023314>.
- [19] Nieh MP, Kučerka N, Katsaras J (2010) Formation mechanism of self-assembled unilamellar vesicles. *Can J Phys* 88:735-740.<https://doi.org/10.1139/P10-014>.
- [20] Petelska AD, Szeremeta M, Kotynska J, Niemcunowicz-Janica A (2021). Experimental and theoretical approaches to describing interactions in natural cell membranes occurring as a result of fatal alcohol poisoning. *Membranes* 11:189. <https://doi.org/10.3390/membranes11030189>.
- [21] Sarfraz M, Afzal A, Yang T, Gai Y, Raza SM, Khan MW, Cheng Y, Ma X, Xiang G (2018). Development of dual drug loaded nanosized liposomal formulation by a reengineered ethanolic injection method and its pre-clinical pharmacokinetic studies. *Pharmaceutics* 10(3):151. <https://doi.org/10.3390/pharmaceutics10030151>.
- [22] Socaciu C, Jessel R, Diehl HA (2000) Competitive carotenoid and cholesterol incorporation into liposomes: effects on membrane phase transition, fluidity, polarity and anisotropy. *Chem Phys Lipids* 106: 79-88. [https://doi.org/10.1016/S0009-3084\(00\)00135-3](https://doi.org/10.1016/S0009-3084(00)00135-3).
- [23] Sun M, Lee J, Chen Y, Hoshino K (2020) Studies of nanoparticle delivery with in vitro bio-engineered microtissues. *Bioact Mater* 5:924-937.<https://doi.org/10.1016/j.bioactmat.2020.06.016>.
- [24] Sut TN, Yoon BK, Park S (2020). Versatile formation of supported lipid bilayers from bicellar mixtures of phospholipids and capric acid. *Sci Rep* 10:13849. <https://doi.org/10.1038/s41598-020-70872-8>.
- [25] Tae H, Park S, Ma GJ (2022). Nanoarchitected air-stable supported lipid bilayer incorporating sucrose–bicelle complex system. *Nano Convergence* 9(3). <https://doi.org/10.1186/s40580-021-00292-5>.

- [26] Truong NP, Whittaker MR, Mak CW, Davis TP (2015) The importance of nanoparticle shape in cancer drug delivery. *Expert Opin Drug* 12:129-142.<https://doi.org/http://dx.doi.org/10.1517/17425247.2014.950564>.
- [27] Van Dam L, Karlsson G, Edwards K (2004) Direct observation and characterization of DMPC/DHPC aggregates under conditions relevant for biological solution NMR. *BBA-Bioenergetics* 1664:241-256. <https://doi.org/10.1016/j.bbamem.2004.06.005>.
- [28] Yang ST, Kreutzberger AJB, Lee J, Kiessling V, Tamm LK (2016). The role of cholesterol in membrane fusion. *Chem Phys Lipids* 199:136-143.<https://doi.org/10.1016/j.chemphyslip.2016.05.003>.
- [29] Zemb T, Dubois M, Deme B, Gulik-Krzywicki T (1999) Self-assembly of flat nanodiscs in salt-free catanionic surfactant solutions. *Science* 283:816-819.<https://doi.org/10.1126/science.283.5403.816>.
- [30] Zhang W, Sun J, He Z (2013). The application of open disk-like structures as model membrane and drug carriers. *Asian J Pharm Sci* 8(3):143-150. <https://doi.org/10.1016/j.ajps.2013.07.019>.
- [31] Zhang X, Barraza KM, Beauchamp JL (2018). Cholesterol provides nonscrificial protection of membrane lipids from chemical damage at air-water interface. *Proc Natl Acad Sci USA* 115(13):3255-3260. <https://doi.org/10.1073/pnas.1722323115>.
- [32] Zhang YT, Shen LN, Zhao JH, Feng NP (2014) Evaluation of psoralen ethosomes for topical delivery in rats by using in vivo microdialysis. *Int J Nanomed* 9:669-678.<https://doi.org/10.2147/IJN.S57314>.